

# Human Body Trajectory Generation Using Point Cloud Data for Robotics Massage Applications

Ren C. Luo, Sheng Y. Chen, Keng. C. Yeh

**Abstract**—Intelligent robot for improving the quality of human life is desirable. To let robot perform the intelligent functions of massage which can serve for humans, adaptive massage trajectory generator is needed to suit for different body shape with different people.

Base on the state of the art human pose recognition techniques, we develop a methodology to build the relationship between camera and human body and generate the specified massage trajectories. Assume we can detect human pose and label each part of human body, we use the RANSAC algorithm to estimate the frontal and sagittal planes and refine it by calculating the minimum moment of inertia of point cloud. The experimental results demonstrate our work which provide a useful method for massage trajectory generation. As an example of service robot application, this method is useful for executing the massage application autonomously.

## I. INTRODUCTION

There have been several applications of health care robot. The DaVinci robot [5] is a telerobotic surgical system which assists doctors to do more precise control for the surgical instruments and has been widely used in the hospital, but doctors have to train up for using the robot system and the price of the robot is also very expensive. The RIBA (Robot for Interactive Body Assistance) robot [9][10][11] has the ability to lift the patients from bed to wheelchair or from wheelchair to bed, and the RP-VITA robot [17] provides the remote presence that doctors or nurses can take care the patients via the remote presence ability as well.

The massage robot has been developed in the previous work [6][7], it used electromyographic (EMG) signals to evaluate the massage effect of multi-finger robot hand. Because there is physical contact between robot and human, the impedance control based multi-finger robot has also been discussed in the work [8].

Although there are few papers which discussed the topic of massage robot, it seldom discusses how to generate the trajectories to adapt different shape of human body. Lu et al. [13] developed a Chinese medical massage robot system, and the robot system tries to find the acupuncture points of the people. But it still relies on the doctor to find the actual



Fig. 1. Dual Arm Robot for Massage Application

acupuncture points and mark it by the colored labels. Wang et al. [14] based on fuzzy set theory to realize the robot massage evaluation system, and the evaluation system displays the three dimensional human shape and marks the acupuncture point of the people in the evaluation systems.

King et al. [4] developed an assistive robot that performs bed bath for patient hygiene autonomously. In their work, the robot mounted the tilting laser range finder and camera in the Cudy robot which can obtain the point cloud of the patient. They provide a user interface in their system that user determine the region of patient they want to clean by the interface. But there is the limitation of the robot which they assume the cleaning region is parallel to the direction of the gravity, so if the patients change the poses on the bed, the methodology sometimes will be hard to propel.

Benefit from the advanced of the robotics perception and sensors, the three dimensional perception has become the most important part of the robot. The point cloud [14] has been widely used in the field of robotics such as object recognition, mapping and path planning. In our work, it is important to know the pose of the humans, and there have been several researches about human skeleton tracking. The most popular approach for skeleton tracking is proposed by Xbox team [15] and Shotton et al. [12], but it has the limitation due to the needs of specific initial pose, and the camera has to be fixed. Buys et al. [2] proposed an adaptable system for RGB-D based human body detection and pose estimation methodology that it gets rid of the limitation of the specific initial pose, and the camera can be moved during the tracking of the skeleton. This paper is based on the human pose recognition methodology which proposed by [2], and we developed a methodology to build the reference

Ren C. Luo is with International Center of Excellence on Intelligent Robotics and Automation Research, National Taiwan University, No. 1, Sec. 4, Roosevelt Road, Taipei, Taiwan 106 renluo@ntu.edu.tw

Sheng Y. Chen is with International Center of Excellence on Intelligent Robotics and Automation Research, National Taiwan University, No. 1, Sec. 4, Roosevelt Road, Taipei, Taiwan 106 sychen@ira.ee.ntu.edu.tw

Keng. C. Yeh is with International Center of Excellence on Intelligent Robotics and Automation Research, National Taiwan University, No. 1, Sec. 4, Roosevelt Road, Taipei, Taiwan 106 kcyeh@ira.ee.ntu.edu.tw

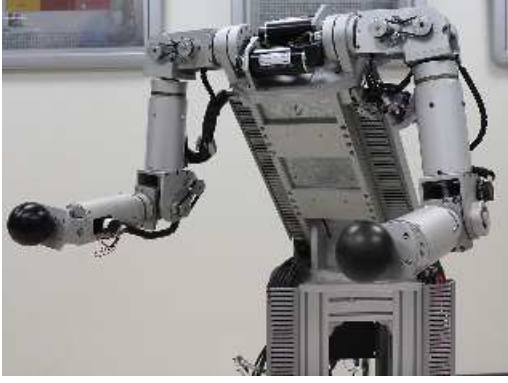


Fig. 2. Dual Arm Robot System developed in NTU-iCeIRA Lab

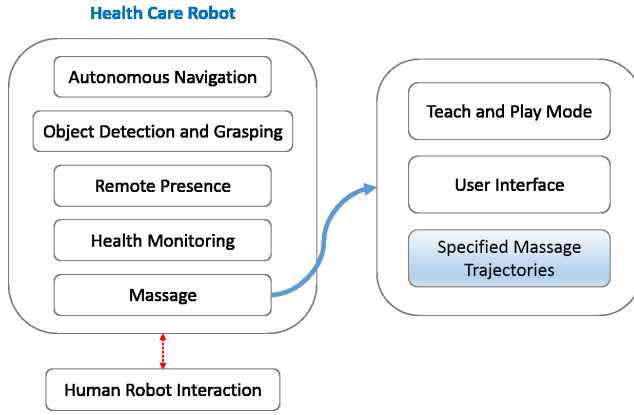


Fig. 3. Functional Block Diagram of Dual Arm Robot for Massage Application

coordinate on the human body which is helpful for executing the massage application autonomously.

The structure of this paper is described as follows: Section II gives a brief structure of the dual arm robot system. Section III illustrates the human pose recognition method which we used in our work. Section IV describes the methodology which we proposed in this paper of massage trajectory planning. The experimental results are shown in Section V. Finally, Section VI concludes our work in this paper.

## II. SYSTEM DESCRIPTION

### A. Hardware Description

The dual arm robot system developed in NTU-iCeIRA Lab for massage application which shown in Figure 2. has 6 degree of freedom on each arm, and there is a linear motor on the bottom of the robot, so that there are totally 13 degrees of freedom in the dual arm robot system in iCeIRA.

The control of the massage robot is based on the real time operating system RTX with 1ms servo control loop on the windows PC. In this paper, we use Microsoft Kinect to acquire the RGB-D data in our dual arm robot system.

### B. Dual Arm Robot with Massage Function

The functional block diagram of dual arm robot is shown in Figure 3. Our work focused on developing the robot

massage function application. There are three mode to execute the massage function. Firstly, people can teach robot to perform the massage movements, robot repeats the taught motion by recording from encoder. Robot then provides a user interface that user can give the desired massage point from the interface. Since the relationship between image and space is known (RGB-D camera), the desired point in the Cartesian space is determined easily.

In order to make robot more intelligent for massage application, robot should have the ability to execute massage function automatically. We proposed a methodology to build a reference coordinate between camera and human body. The relationship will help robot repeat the massage trajectories with a reference coordinate. To achieve this function, the following sections will illustrate the methodology we proposed.

## III. HUMAN POSE RECOGNITION

In this paper, we use the approach to recognize both human pose and each body parts which is proposed by Buys et al. [2]. This approach views the recognition of human pose and each body parts problem as the object recognition problem; it first segments human body to several parts: head parts (top and bottom face), neck part, chest parts, hip parts, arm parts, elbow parts, forearm parts, hand parts, thigh parts, knee parts, leg parts and foot parts. Each part is divided into right and left parts except neck. The pose recognition process computes all of the pixels which came from the depth camera. All the pixels passed through a classifier and recognized to which body parts they belonged. The classifier includes three processes: Database building, depth image feature deriving and randomized decision forests classifying, which are illustrated briefly as below:

### A. Database Building

To build the database, the training data is necessary. In this case, the training data which is point cloud of human body shape is created by computer graphics and real human tracking techniques (Base character, pose, rotation and translation, hair and clothing, camera position and orientation). Furthermore, some weight and height variation and camera noise are added. Then every training data are labeled each body parts as described above.

### B. Depth Image Features

The depth image is defined to identify each body parts different characteristic. It is like the feature extraction techniques such as SIFT and SURF in image process, but here the data is depth data. The depth image feature is defined as follow:

$$f_{\phi}(I, x) = d_I(x + \frac{u}{d_I(x)}) - d_I(x + \frac{v}{d_I(x)}) \quad (1)$$

Where  $d_I(x)$  represents the depth value of pixel  $x$  in depth image. The parameters  $\phi = (u, v)$  are offset parameters which should be defined. The term  $\frac{1}{d_I(x)}$  is the normalization factor which ensures the feature is depth invariant.



Fig. 4. Human Pose Recognition

#### IV. RANDOMIZED DECISION FORESTS CLASSIFICATION

The randomized decision forests (RDF) are created to classify the pixel belongs which part. Each split node in the forests consists of feature  $\phi$  and threshold  $\tau$ . The forests are kind of binary tree, the current node is updated to left or right child node is according to the comparison of  $f_\phi(I, x)$  and  $\tau$ . Finally the node will reach the last leaf which the leaves consist of the label  $c$  of different human body parts as described above, then the learned distribution  $P_t(c, I, x)$  are stored as the result of the  $t$ -th tree. The final distribution combines all the results of each tree:

$$P(c|I, x) = \frac{1}{T} \sum_{t=1}^T P_t(c|I, x) \quad (2)$$

Here  $T$  is the number of created randomized decision forests.

In our work, we assume the human pose estimation which we used is reliable. The result of human pose estimation is shown as Figure 4. Once the relation has been found, the reference coordinate on the human body has been specified as well. It gives robot a reference to repeat the specified trajectories which designed by designers for massage purpose.

#### V. MESSAGE TRAJECTORY GENERATION

In this section, we illustrate the methodology of message trajectory generating. Based on the work proposed by Buys et al. [2], the human body is divided into 30 parts, but we simplified it into 5 parts in our application. Besides, there are two main parts of the human body which we used are the head and torso parts.

##### A. Determination of Frontal and Sagittal Planes

For the object of generating the message trajectory on the human body, the relationship between human and robots sensor has to be obtained. Once the transformation in the space is known, the designed message trajectories can be repeated for executing specific massage motions.

At the first, we find the frontal and sagittal planes of the human which both their definitions are shown as Figure 5.

Because the information of each part of the human is known after human pose recognition process, the region of

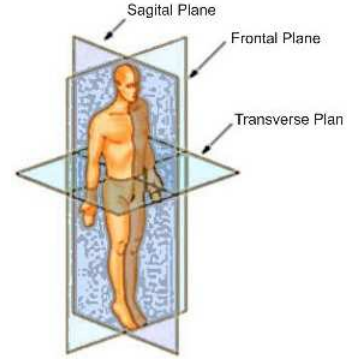


Fig. 5. Diagram Showing Sagittal, Frontal and Transverse Planes [16]

interest of the torso of people is determined by (3)(4), and we estimate the frontal plane equation by using RANSAC algorithm [3].

$$\text{left top corner of ROI} = \min\{u, v | l_i \in l_{torso}\} \quad (3)$$

$$\text{right bottom corner of ROI} = \max\{u, v | l_i \in l_{torso}\} \quad (4)$$

Where  $l_i$  represents the label on the image with coordinate  $(u, v)$ , and  $l_{torso}$  represents the label of torso part which contains the hip and chest part with both sides.

After the determination of frontal plane, the border of right and left torso is extracted to be candidate points which is used to determine the sagittal plane of the people.

$$p_c = \{l_i | l_i \in l_{Ltorso} \text{ \& } l_i \text{ is the neighbor of } l_{Rtorso}\} \quad (5)$$

Where  $l_{Ltorso}$  and  $l_{Rtorso}$  represent the label of left and right torso parts and here we adopt the 4-neighbor definition.

The candidate points  $p_c$  will be projected onto the frontal plane to make sure candidate points lie on the frontal plane. The projected  $p_c$  is notated as  $p_{cp}$ . The candidate points  $p_{cp}$  are used to estimate the intersection line  $l_{sf}$  between frontal and sagittal planes by RANSAC algorithm. Once  $l_{sf}$  is determined, the normal vector of sagittal plane  $n_s$  is the cross product of  $l_{sf}$  and the normal vector  $n_f$  of frontal plane.

$$n_s = l_{sf} \times n_f \quad (6)$$

##### B. Coordinate Transformation

The camera coordinate can be transformed to human body coordinate by using the normal vectors of frontal and sagittal planes as the references. The transformation equation is:

$$p'_{human \text{ body}} = R_{3 \times 3} \cdot p_{camera} + T_{3 \times 1} \quad (7)$$

Where  $R_{3 \times 3}$  is the rotation matrix and  $T_{3 \times 1}$  is the translation matrix,  $p'_{human \text{ body}}$  and  $p_{camera}$  are the vectors which represent the point cloud data with  $[x \ y \ z]^T$  in human body and camera coordinates.

The rotation matrix can be obtained by the relationship of normal vector of sagittal and transverse planes and camera coordinate as Fig. 6. Where,

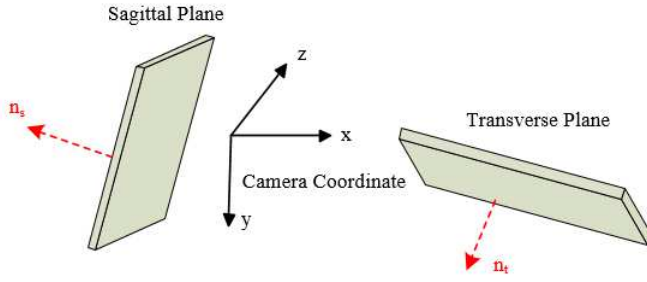


Fig. 6. Relationship of Camera and Human Body Coordinate

$$n_t = n_s \times n_f \quad (8)$$

The camera coordinate has to be rotated twice to let the human body coordinate coincide with camera coordinate. First, it rotates the angle  $\beta$  along y-axis between x-axis of camera coordinate and normal vector  $n_s$  with rotation matrix  $R_y$ , and then the  $n_t$  becomes to  $n'_t$  as (9)

$$n'_t = R_y n_t \quad (9)$$

And then, the camera coordinate rotates the angle  $\gamma$  between y-axis of camera coordinate and normal vector  $n'_t$  along x-axis with rotation matrix  $R_x$ . Where,

$$R_x = \begin{bmatrix} \cos\gamma & -\sin\gamma & 0 \\ \sin\gamma & \cos\gamma & 0 \\ 0 & 0 & 1 \end{bmatrix}, R_y = \begin{bmatrix} \cos\beta & 0 & \sin\beta \\ 0 & 1 & 0 \\ -\sin\beta & 0 & \cos\beta \end{bmatrix}$$

Hence, the equation (7) could be reformed to equation (10) and (11)

$$p''_{humanbody} = R_y \cdot p_{camera} \quad (10)$$

$$p'_{humanbody} = R_x \cdot p''_{humanbody} + T \quad (11)$$

And the translation matrix T can be obtained by arbitrary choosing the point in  $p_{cp}$ . In our work, we choose the point p with maximum y value.

### C. Find the Principle Plane of the Back

In consideration of the back of human is not always straight and the view angle of camera is not fixed in practice, the plane estimation by RANSAC algorithm could have a larger angle of inclination along x-axis. To refine the frontal plane fulfilling the tendency of angle with minimum moment of inertia, we find the principle plane of the back which satisfied the condition to adjust the reference coordinate. Because the estimated frontal plane is perpendicular to the sagittal plane, we fine tune the angle along x-axis by calculating the projected point on the sagittal plane. Take advantage of coordinate transformation, all the points  $p_{humanbody}$  of the torso project onto the transformed sagittal plane (y-z plane) and the axis of minimum moment of inertia is regarded as the principle axis. To find the minimum moment of inertia of the point cloud, the principle axis is modeled as the parameter

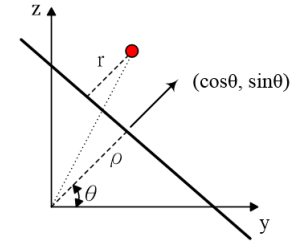


Fig. 7. Finding the Principal Plane from Point Cloud

of  $\rho$  and  $\theta$  in the polar coordinate in Fig. 7. Since the dot product of the normal vector of line and the distance  $r$  which is shown in Fig. 7 is zero. The equation of the moment of inertia can be expressed as (12)

$$\Gamma^2 = a \cos^2 \theta + b \sin \theta \cos \theta + c \cos^2 \theta \quad (12)$$

Where

$$a = \sum_{i=1}^n (y'_i)^2 S_{i,j}, b = 2 \sum_{i=1}^n \sum_{j=1}^m (y'_i)(z'_j) S_{i,j}, c = \sum_{j=1}^m (z'_j)^2 S_{i,j}$$

and

$$y' = y - \bar{y}, z' = z - \bar{z}$$

The equation (12) can be expanded as (13) by double angle formula.

$$\Gamma^2 = \frac{1}{2}(a+c) + \frac{1}{2}(a-c)\cos 2\theta + \frac{1}{2}b\sin 2\theta \quad (13)$$

Take derivative of equation (13), so when

$$\frac{d\Gamma^2}{d2\theta} = 0 \quad (14)$$

We get equation (15) to obtain  $\theta$  and  $\theta \in [-90^\circ, 90^\circ]$

$$\tan 2\theta = \frac{b}{a-c} \quad (15)$$

There are two solutions which could be the maximum or minimum values, and we take another derivative of equation (15), that is

$$\frac{d}{d2\theta} \frac{d\Gamma^2}{d2\theta} = 0 \quad (16)$$

And it returns equation (17)

$$\tan 2\theta = \frac{a-c}{b} \quad (17)$$

If equation (17)  $> 0$ , there is the minimum value of moment of inertia of the point cloud, and if equation (17)  $< 0$ , there is the maximum value.

And the point cloud is rotated with the angle  $\theta$  along the x-axis.

$$p_{humanbody} = R \cdot p'_{humanbody} \quad (18)$$

Here,



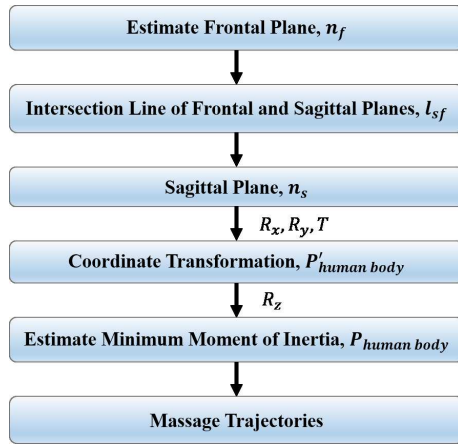


Fig. 8. Flowchart of Massage Trajectory Generation

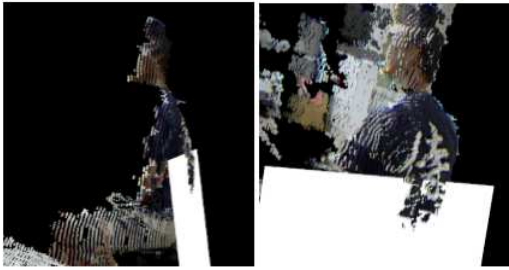


Fig. 9. Estimation of Frontal Plane



Fig. 10. Estimation of Sagittal Plane

$$R = \begin{bmatrix} \cos\theta & -\sin\theta & 0 \\ \sin\theta & \cos\theta & 0 \\ 0 & 0 & 1 \end{bmatrix}$$

#### D. Trajectory Generating

In previous steps, we found a reference coordinate for designing the massage trajectory, and the flowchart of each step is summarized in Fig. 8. We project all points onto the x-y plane and the intersection of frontal and sagittal planes is the symmetric line of the back. The trajectory can be designed on the reference plane and re-project the designed trajectories which on the reference to the point cloud in the space.



Fig. 11. Vertical Trajectory (Red Line)



Fig. 12. Horizontal Trajectory (Green Line)

## VI. EXPERIMENTAL RESULTS

There are many manipulation ways for massage therapy, such as press, push, rub, knock, roll, pinch and etc... Some massage methods need the target point to start the massage function of the robot, and some massage methods need a section of trajectory to execute the massage movement like push with a long distance or rub on the specific region of body.

To verify the proposed methodology is workable on massage trajectory generation, we design three specified trajectory include: vertical and horizontal trajectories for push movement, and circle trajectory for rub movement.

In our experiments, we try to find the trajectory which lies on the either sides of the backbone which there are many acupuncture points in Chinese medical theorem and bilateral



Fig. 13. Circle Trajectory (Yellow Line)

back of human. By the series of transformations in the space, we can simply design the trajectories on the x-y plane of human body coordinate.

The Fig. 9 shows the estimation of frontal plane and Fig. 10 shows the estimation of sagittal plane. Fig. 11 shows the vertical trajectories which we design on the x-y plane is  $x = \pm 0.05$  meters. Fig. 12 shows the horizontal trajectory on human back for push movement of massage. Fig. 13 shows the circle trajectory on human back which is designed for rub movement.

## VII. CONCLUSION

In our work, we propose the methodology to generate the massage trajectory by the RGB-D sensor. By the definition and finding the frontal and sagittal planes, the point cloud can be transformed on the reference plane which is useful to design the massage trajectories on the human body.

The experimental results demonstrate our work which provide a useful method for massage trajectory generation. As an example of service robot application, this method is useful for executing the massage application autonomously.

## REFERENCES

- [1] A. Aldoma, Z.-C. Marton, F. Tombari, W. Wohlkinger, C. Potthast, B. Zeisl, et al., "Tutorial: Point Cloud Library: Three-Dimensional Object Recognition and 6 DOF Pose Estimation," *Robotics and Automation Magazine, IEEE*, vol. 19, pp. 80-91, 2012.
- [2] K. Buys, C. Cagniat, A. Baksheev, T. De Laet, J. De Schutter, and C. Pantofaru, "An adaptable system for RGB-D based human body detection and pose estimation," *Journal of Visual Communication and Image Representation*, 2013.
- [3] M. A. Fischler and R. C. Bolles, "Random sample consensus: a paradigm for model fitting with applications to image analysis and automated cartography," *Communications of the ACM*, vol. 24, pp. 381-395, 1981.
- [4] C.-H. King, T. L. Chen, A. Jain, and C. C. Kemp, "Towards an assistive robot that autonomously performs bed baths for patient hygiene," in *Intelligent Robots and Systems (IROS)*, 2010 IEEE/RSJ International Conference on, 2010, pp. 319-324.

- [5] J. Leven, D. Burschka, R. Kumar, G. Zhang, S. Blumenkranz, X. D. Dai, et al., "DaVinci canvas: a telerobotic surgical system with integrated, robot-assisted, laparoscopic ultrasound capability," in *Medical Image Computing and Computer-Assisted Intervention?MICCAI 2005*, ed: Springer, 2005, pp. 811-818.
- [6] R. C. Luo and C.-C. Chang, "Electromyographic signal integrated robot hand control for massage therapy applications," in *Intelligent Robots and Systems (IROS)*, 2010 IEEE/RSJ International Conference on, 2010, pp. 3881-3886.
- [7] R. C. Luo and C. C. Chang, "Electromyographic evaluation of therapeutic massage effect using multi-finger robot hand," in *Robotics and Automation (ICRA)*, 2011 IEEE International Conference on, 2011, pp. 2431-2436.
- [8] R. C. Luo, C. C. Chang, and Y.-W. Perng, "Impedance control on a multi-fingered robot hand based on analyzed electromyographic information for massage applications," in *Industrial Electronics, 2009. ISIE 2009. IEEE International Symposium on*, 2009, pp. 1228-1233.
- [9] T. Mukai, S. Hirano, H. Nakashima, Y. Kato, Y. Sakaida, S. Guo, et al., "Development of a nursing-care assistant robot riba that can lift a human in its arms," in *Intelligent Robots and Systems (IROS)*, 2010 IEEE/RSJ International Conference on, 2010, pp. 5996-6001.
- [10] T. Mukai, S. Hirano, M. Yoshida, H. Nakashima, S. Guo, and Y. Hayakawa, "Tactile-based motion adjustment for the nursing-care assistant robot RIBA," in *Robotics and Automation (ICRA)*, 2011 IEEE International Conference on, 2011, pp. 5435-5441.
- [11] T. Mukai, S. Hirano, M. Yoshida, H. Nakashima, S. Guo, and Y. Hayakawa, "Whole-body contact manipulation using tactile information for the nursing-care assistant robot riba," in *Intelligent Robots and Systems (IROS)*, 2011 IEEE/RSJ International Conference on, 2011, pp. 2445-2451.
- [12] J. Shotton, T. Sharp, A. Kipman, A. Fitzgibbon, M. Finocchio, A. Blake, et al., "Real-time human pose recognition in parts from single depth images," *Communications of the ACM*, vol. 56, pp. 116-124, 2013.
- [13] L. Shouyin, G. Huanbing, L. Cungen, and W. Tao, "Design of Chinese medical massage robot system," in *Electrical and Control Engineering (ICECE)*, 2011 International Conference on, 2011, pp. 3882-3885.
- [14] T. Wang, T. Bei, and Y. Li, "Research and realization of the robot massage evaluation system based on fuzzy set theory," in *Intelligent Control and Automation (WCICA)*, 2010 8th World Congress on, 2010, pp. 6498-6501.
- [15] Microsoft XBOX Kinect, 2010, <http://xbox.com>
- [16] "Sagittal Plane," <http://www.wikipedia.org>
- [17] InTouch Technologies, <http://www.intouchhealth.com>